Theory of chemically induced dynamic electron polarization. I*

J. Boiden Pedersen† and Jack H. Freed
Department of Chemistry, Cornell University, Ithaca, New York 14850
(Received 13 October 1972)

A general and detailed analysis is given of the phenomenon of chemically-induced dynamic electron polarization (CIDEP) by means of the stochastic-Liouville method in accordance with the earlier preliminary report. The finite-difference technique employed permits rapid and convergent solutions without requiring any untoward assumptions on the nature of the models. The dependence of the polarization on the exchange interaction $J(r)$, the Larmor frequency differences between the interacting pair of radicals, diffusion rates, and rates of spin-selective chemical reactions are given in detail. It is shown that models in which $J(r)$ is taken to decay exponentially with r, the radical-separation distance of the radical pair, yield results which are distinctly different from those for a contact exchange model, when J_0 [the value of $J(r)$ when r is at the distance of closest approach] is appreciable. The former, more realistic model yields substantial polarizations asymptotically independent of J_0, but larger the slower the decrease of $J(r)$ with r; the contact exchange model, however, rapidly goes to zero with increasing J_0. These asymptotic values of polarization are predicted to be as high as 10–40 times the equilibrium polarizations (P_{eq}) for sensible values of the relevant parameters, while for values of J_0 yielding maximum polarizations (generated at the formative reaction), they can be greater than 100 P_{eq}. These results are of the correct order for agreement with recent experiments. The polarizations have been related to the CIDEP intensities that one may observe for typical schemes of radical production, reaction, and relaxation in order to allow a comparison of the theoretical predictions with experiment.

I. INTRODUCTION

Recently we have called attention[1] to the fact that it is possible to develop a rigorous analysis of the interesting new phenomenon of chemically induced dynamic electron polarization (CIDEP) by means of the stochastic-Liouville method,[2,3] and we presented a preliminary account[1] of our results, which showed that for reasonable models it was possible to predict substantial polarizations. In this report, we present a detailed account of our theoretical methods and results on CIDEP.

The stochastic-Liouville method,[2,3] is a method whereby one may simultaneously include the details of the spin interactions and dynamics, represented in a proper spin Hamiltonian, as well as the classical stochastic behavior of the motions of the spin-containing radicals in liquids including, when necessary, spin-selective chemical reactions. In the sense of simultaneously including both dynamical and stochastic parts, it bears a formal similarity to the Boltzmann equation in the kinetic theory of gases.

There have been several earlier attempts to analyze CIDEP[4–9] in terms of the combined effects of an exchange interaction between a radical pair formed from a dissociating molecule and Larmour frequency differences between the two radicals. The primary feature of all approaches is that the relative motion of the two radicals will modulate the short-range exchange interaction.[3] However, the difficulty of including this latter feature has resulted in the use of simplifying approximations such as the consideration of just the lifetime of a single encounter,[4] adiabatic-crossing-type models,[5,6] or the effects of a radical–radical re-encounter.[7] We have already pointed out[1] that all these are submodels of the complete dynamics, whereby the motion modulates the exchange interaction and polarization is developed; and it is the complete dynamics, without untoward simplifying assumptions, that is explicitly included in a rigorous solution to the stochastic-Liouville equation.

In our desire to formulate the model of an exchanging and diffusing radical pair in such a manner as to be consistent with reasonable physical expectations, we found that we could avoid undue approximations most conveniently by seeking finite-difference solutions to the stochastic-Liouville expressions. That is, we have been able to obtain complete and rigorous solutions for reasonable models of the exchange interaction and its spatial extent (e.g., an exponential decrease with distance) and the diffusion at the price of numerical (but very rapid) computer solutions. Our quantitative predictions should then be very useful to the experimenter as well as a standard for comparison with other more approximate approaches. In general, we find that our complete solutions are more complex in detail than any of the approximate earlier models, although that of Adrian[7] provides useful, but not quantitative, insights.

In Sec. II we discuss our theoretical method including the stochastic-Liouville equation, the basic models, and the finite difference methods. Our results are presented and discussed in Sec. III. The relationship between the CIDEP polarizations calculated by the methods of Sec. II for individual collisions and actual CIDEP intensities that may be observed in an experi-

ment is discussed in Sec. IV along with a comparison with recent experiments. A summary and conclusions appear in Sec. V.

II. THEORETICAL APPROACH

A. Stochastic-Liouville Equation

The basic equation describing the spin dynamics of radicals under the combined effects of spin interactions and diffusion in liquid solution is the stochastic-Liouville equation given in terms of the spin-density matrix $\rho(\mathbf{r}_i, t)$[2,3]:

$$\partial\rho(\mathbf{r}_i, t)/\partial t = -i\mathcal{H}^x(\mathbf{r}_i)\rho(\mathbf{r}_i, t) + D\Gamma_r\rho(\mathbf{r}_i, t). \quad (2.1)$$

In this equation $\mathcal{H}^x(\mathbf{r}_i)$ is the Liouville operator associated with the spin Hamiltonian $\mathcal{H}(\mathbf{r}_i)$ (i.e., for any two operators A and B, $A^xB \equiv [A, B]$). We shall consider the interaction of a radical pair ab, so we may write

$$\mathcal{H}(\mathbf{r}_i) = \mathcal{H}^0(\mathbf{r}_a, \mathbf{r}_b) + \mathcal{H}', \quad (2.2)$$

where $\mathcal{H}^0(\mathbf{r}_a, \mathbf{r}_b)$ is that part of $\mathcal{H}(\mathbf{r}_i)$ that is diagonal in a basis set of coupled electron spins (i.e., singlet-triplet representation). It is given by

$$\mathcal{H}^0(\mathbf{r}_a, \mathbf{r}_b) = \tfrac{1}{2}(g_a+g_b)\beta_e\hbar^{-1}B_0(S_{az}+S_{bz}) + \tfrac{1}{2}(\sum_j^a A_j\mathbf{I}_j + \sum_k^b A_k\mathbf{I}_k)(\mathbf{S}_a+\mathbf{S}_b) - J(\mathbf{r}_a, \mathbf{r}_b)(\tfrac{1}{2}+2\mathbf{S}_a\cdot\mathbf{S}_b). \quad (2.3)$$

The off-diagonal part $\mathcal{H}'$ of $\mathcal{H}(\mathbf{r})$ is independent of $\mathbf{r}$ and is given by

$$\mathcal{H}' = \tfrac{1}{2}(g_a-g_b)\beta_e\hbar^{-1}B_0(S_{az}-S_{bz}) + \tfrac{1}{2}(\sum_j^a A_j\mathbf{I}_j - \sum_k^b A_k\mathbf{I}_k)(\mathbf{S}_a-\mathbf{S}_b). \quad (2.4)$$

Equation (2.4) expresses the fact that $\mathcal{H}'$ consists only of differences in g values and hyperfine energies between the two interacting radicals. $J(\mathbf{r}_a, \mathbf{r}_b)$ in Eq. (2.3) is the exchange interaction between radicals a and b, which depends explicitly on $\mathbf{r}_a$, $\mathbf{r}_b$ (or more meaningfully on $\mathbf{r}$, the radial distance between the radicals as well as their relative orientations). We have neglected in Eqs. (2.2)–(2.4) any intramolecular anisotropic $\mathbf{g}$ or $\mathbf{A}$ tensor contributions, which tend to average out in liquids in times of the order of 10^{-10}–10^{-11} sec. While this is not rigorous, any effects from incomplete averaging should represent small corrections to the g_a, g_b, A_a, and A_b used in Eqs. (2.3) and (2.4). We also neglect spin–rotational terms, since spin–rotational relaxation is even faster, $\tau_J \lesssim 10^{-12}$ sec. We have also neglected relaxation due to intermolecular electron–electron dipolar interactions, which, like $J(\mathbf{r}_a, \mathbf{r}_b)$ are modulated by the relative translation diffusion of the radicals. In neglecting dipolar interactions, we are guided somewhat by the fact that for free radicals in normal liquids, the exchange mechanism usually predominates in the concentration-dependent spin relaxation. The explicit relaxation effects of these terms may be included at another stage in the analysis (cf. Sec. IV), and we are only neglecting any direct effects they may have on the polarization process. We further assume, for simplicity, that $J(\mathbf{r}_a, \mathbf{r}_b) = J(r)$, i.e., the exchange interaction is independent of the relative molecular orientations and depends only upon radical distance r. Also in the analysis of high-field experiments we need only consider the secular $A_jI_{jz}S_{az}$-type terms.

The operator $D\Gamma_r$ in Eq. (2.1) is the diffusion operator for the relative diffusion between radicals a and b, i.e., the diffusion in the intermolecular vector $\mathbf{r}$. This may be taken to be a normal Brownian diffusion process (a Wiener–Einstein process) with diffusion coefficient $D = D_a + D_b$, i.e., the sum of the individual diffusion coefficients. This amounts to neglecting any spin-dependent effects on the diffusive motion, which should be a good assumption when $\hbar\,|\,J(r)\,| < kT$.[10]

The diffusion operator Γ_r can be written in spherical polar coordinates as

$$\Gamma_r = \Gamma_r + (1/r^2)\Gamma_\Omega, \quad (2.5)$$

where Γ_r, the radial part, is given by

$$\Gamma_r = (1/r^2)(\partial/\partial r)r^2(\partial/\partial r) \quad (2.6)$$

while the angular part Γ_Ω is

$$\Gamma_\Omega = (\sin\theta)^{-1}(\partial/\partial\theta)[\sin\theta(\partial/\partial\theta)] + (\sin^2\theta)^{-1}(\partial^2/\partial\phi^2). \quad (2.7)$$

Our above assumptions effectively allow us to write $\mathcal{H}(\mathbf{r}_a, \mathbf{r}_b) \to \mathcal{H}(r)$, so one may integrate out the angular dependence (of θ and ϕ) in Eq. (2.1) leaving a stochastic-Liouville expression for[11]

$$\rho(r, t) = \int_0^\pi d\theta \sin\theta \int_0^{2\pi} d\phi\rho(\mathbf{r}, t) \quad (2.8)$$

given by

$$\partial\rho(r, t)/\partial t = -i\mathcal{H}^x(r)\rho(r, t) + D\Gamma_r\rho(r, t). \quad (2.9)$$

The Laplace transform of Eq. (2.9) is

$$s\hat{\rho}(r, s) - \hat{\rho}_0(r) = -i\mathcal{H}^x(r)\hat{\rho}(r, s) + D(\partial^2/\partial r^2)\hat{\rho}(r, s), \quad (2.10)$$

where

$$\hat{\rho}(r, s) \equiv \int_0^\infty e^{-st}r\rho(r, t)dt \quad (2.11)$$

and $\hat{\rho}_0(r) = r\rho(r, 0)$ gives the initial condition. Equation (2.10) is an equation in only the single spatial variable r *as well as* in the spins of the radical pair. One could solve Eq. (2.10) by expanding $\hat{\rho}(r, s)$ in eigenfunctions of the diffusion operator[2,3] (viz. a spherical Bessel function expansion). However we have found it

more convenient to employ a finite difference technique. That is, one writes[12a]

$$\partial^2\hat{\rho}(r,s)/\partial r^2=(1/\Delta r^2)[\hat{\rho}(r-\Delta r,s) -2\hat{\rho}(r,s)+\hat{\rho}(r+\Delta r,s)], \quad (2.12)$$

where Δr is a small, but finite, increment in r. In principle, one must take Δr small enough to properly represent the functions varying in r. In our case $J(r)$ is the most rapidly varying function of r and this method allows us to consider a wide range of functional dependences of J with r.

B. Polarizations

The time-dependent polarization of radical a, or $P_a(t)$, is given by

$$P_a(t)=-2\,\mathrm{Tr}\{\rho(t)S_{az}\}, \quad (2.13a)$$

where the sign convention yields positive equilibrium polarizations P_{eq} and where

$$\rho(t)\equiv\int_0^\infty r^2\rho(r,t)dr. \quad (2.13b)$$

The Laplace transform of $P_a(t)$ is then given by

$$\hat{P}_a(s)=-2\,\mathrm{Tr}\left[\int_0^\infty r\hat{\rho}(r,s)dr S_{az}\right]. \quad (2.14)$$

It is easy to see, by writing $2S_{az}=(S_{az}-S_{bz})+(S_{az}+S_{bz})$, that Eq. (2.13) is

$$P_a(t)=-[\rho_{ST_0}(t)+\rho_{T_0S}(t)] +[\rho_{T_-T_-}(t)-\rho_{T_+T_+}(t)] \quad (2.15a)$$

while

$$P_b(t)=+[\rho_{ST_0}(t)+\rho_{T_0S}(t)] +[\rho_{T_-T_-}(t)-\rho_{T_+T_+}(t)]. \quad (2.15b)$$

In Eq. (2.15) S, T_0, and $T_\pm$ refer to the standard singlet and triplet states of the radical pair, while ρ_{AB} refers to the ABth matrix element of ρ.[13] One notes from Eqs. (2.15), that the first bracketed terms yield opposite polarizations for radicals a and b, while the second bracketed terms give identical polarizations. In the high-field approximation the form of Eq. (2.4) means that only S and T_0 states couple to give induced polarizations, while $T_\pm$ states remain unchanged (cf. Sec. II.D).

One notes that the initial condition must be specified to solve Eq. (2.10). The precise initial conditions one utilizes depends on the specific physical model appropriate to the experiment. Thus, for example, one may have a chemical reaction that produces radical pairs initially in pure singlet (or pure triplet) states. Then the stochastic-Liouville equation (2.9) or (2.10) is solved subject to this initial condition, e.g., $\rho_0(r)_{SS}=\delta(r-r_0)/r_0^2$, where r_0 is the initial separation. Alternatively, the polarization may be conceived of as being generated whenever independently produced radicals approach one another and have a finite probability of reacting. The initial conditions here would then involve equal populations in the S and T_0 states, which is a direct consequence of (1) having equal initial populations of states $+a$, $-b$ and $-a$, $+b$ and (2) having random initial phases, i.e., $\rho_{\pm a,\mp b,\mp a\pm b}(t=0)=0$, etc.

Thus, the polarization transform $\hat{P}_a(s)$ may be obtained from Eqs. (2.10)–(2.12), (2.14), and the Laplace transform of Eq. (2.15a) once the appropriate initial conditions are chosen. Then $P_a(t)$ is recovered by inverse transformation. However, we shall find that we need just the limiting value of $P_a(t)$ as $t\to\infty$, which is, according to the well-known equality,[14]

$$P_a^\infty\equiv\lim_{t\to\infty}P_a(t)=\lim_{s\to0}s\hat{P}_a(s). \quad (2.16)$$

In the high-field approximation, when the $T_\pm$ states do not contribute to the induced polarization, then one has

$$P_a^\infty=-2\lim_{s\to0}s\int_0^\infty r\,\mathrm{Re}[\hat{\rho}_{ST_0}(r,s)]dr. \quad (2.17)$$

C. Stochastic Matrix and Boundary Conditions

The application of the finite difference technique,[12a] expressed by Eq. (2.12), is essentially equivalent to transforming the continuous diffusion equation (a Fokker–Planck equation) into a discrete Master equation involving a transition-probability matrix $\mathbf{W}$,[12b] coupling $\rho(r,t)$ between discrete values $\rho(r_0+j\Delta r,t)$ where $j=0,1,2,\cdots,N$. These discrete values form a column vector $\boldsymbol{\rho}$. Thus

$$D(\partial^2\hat{\rho}/\partial r^2)\to\mathbf{W}\hat{\boldsymbol{\rho}}. \quad (2.18)$$

If we let $r_0=d$ be the distance of closest approach, and if we do not allow any net accumulation of radicals at this point, then this establishes a boundary condition, which is formally equivalent to a reflecting wall.[12a] This condition is

$$\partial\rho(r,t)/\partial r]_{r=d}=0 \quad (2.19a)$$

or equivalently

$$\partial\hat{\rho}(r,s)/\partial r]_{r=d}-[\hat{\rho}(d,s)/d]=0. \quad (2.19b)$$

In finite difference notation, Eq. (19b) becomes

$$\{[\hat{\rho}(d+\Delta r,s)-\hat{\rho}(d-\Delta r,s)]/2\Delta r\} -[\hat{\rho}(d,s)/d]=0. \quad (2.19c)$$

Then for $r=d$ Eq. (2.12) gives

$$D\partial^2\hat{\rho}(r,s)/\partial r^2]_{r=d}\to(D/\Delta r^2) \times\{-2[1+(\Delta r/d)]\hat{\rho}(d,s)+2\hat{\rho}(d+\Delta r,s)\}, \quad (2.20)$$

where we have now eliminated the $\rho(d-\Delta r)$ term.

In order to make the calculation tractable, one must

limit the space to a finite region, the outer limit of which is given by $r_N=r_0+N\Delta r$. A choice of the value of r_N is guided by two considerations: (1) it must be large enough that particles separated by r_N exert an exchange interaction $J(r_N)=0$; (2) the probability $y_{N,K}$ is small that particles separated by r_N will diffuse close enough (i.e., to r_K) such that $J(r_K)$ is nonnegligible. One has $y_{N,K}=r_K/r_N$.[15] This second condition is needed to permit re-encounters of the radical pair. It is clear that a reflecting barrier at r_N would induce physically unjustified extra encounters (especially as $t\longrightarrow\infty$!). But an absorbing wall may be satisfactorily employed, since, as r_N becomes large, the fraction of the re-encounters not included becomes negligible. [Note that Condition (2) is appropriate only for very dilute solutions. More moderate radical concentrations would probably require r_N chosen as the mean distance between successive radical–radical encounters and some adjustment is made in Sec. III for faster diffusion rates.] Thus, as $t\longrightarrow\infty$ the radical pair achieves unit probability of being separated by $r_N\gg r_0$.

We now adopt the notation of writing $\hat{p}(r_0+j\Delta r, s)$ as $\hat{p}(j, s)$ and a transition-probability matrix element of $\mathbf{W}$ in Eq. (2.18) as $W_{r_0+j\Delta r\rightarrow r_0+k\Delta r}$ as $W_{k,j}$. Then the absorption condition at $r=r_N$ is

$$W_{n,n}=W_{n-1,n}=0. \tag{2.21}$$

The total $\mathbf{W}$ is then given as a tridiagonal matrix:

$$\frac{D}{\Delta r^2}\begin{pmatrix} -2[1+(\Delta r/d)] & +2 & & & & & \\ 1 & -2 & 1 & & & & \\ & 1 & -2 & 1 & & & \\ & & \cdot & \cdot & \cdot & & \\ & & & \cdot & \cdot & \cdot & \\ & & & & 1 & -2 & 1 \\ & & & & & 1 & -2 & 0 \\ & & & & & & 2 & 0 \end{pmatrix}, \tag{2.22}$$

where the last row has been determined by the conservation of total probability requirement (see below).

Note now that in the finite difference technique we approximate the integral in Eq. (2.14) for $P_a(s)$ as

$$\int_0^\infty r\hat{p}(r, s)dr=\sum_{i=1}^{N} V(i)\hat{p}(i, s), \tag{2.23}$$

where $V(i)$ is the radial weighting factor for the r_ith position. Specifically one has

$$\begin{aligned} &V(0)=d\Delta r/2 \\ &V(i)=r_i\Delta r \qquad \text{for } 0<i<N \\ &V(N)=r_N\Delta r/2. \end{aligned} \tag{2.24}$$

Now the diffusion equation in the absence of spin-dependent phenomena, is of course

$$d\hat{p}(r, t)/dt=\Gamma_r\hat{p}(r, t)\longrightarrow\mathbf{W}\hat{p}(r, t), \tag{2.25}$$

where $\hat{p}(r, t)=rp(r, t)$, and $p(r, t)$ is the classical probability density. The arrow in Eq. (2.25) just reflects the passage to a finite difference expression [cf. Eq. (2.18)]. Then the conservation of probability[12b] condition becomes

$$\sum_{i=0}^{N} V(i)W_{i,j}=0 \qquad \text{for } j=0, 1, \cdots, N. \tag{2.26}$$

That is, the weighted sum of elements of $\mathbf{W}$ for each column must be zero. The $\mathbf{W}$ matrix given by Eq. (2.22) is seen to be in accordance with Eq. (2.26).

There is a convenient way to keep r_N large enough to satisfy the above two conditions, while having Δr small enough to be converging to the correct solution and yet to keep N from getting too large. In the region where $J(r)\neq 0$ one has $r_0\leq r\leq r_M$ with $r_M\ll r_N$. In this region Δr must be chosen small enough compared to the variation in $J(r)$. However, for $r_M\leq r\leq r_N$, where $J(r)=0$, Δr can be taken much larger and still adequately describe just the Brownian diffusion. We take the Δr in the latter region as f times larger than that of the former region (where $f\sim 10$). Then Eq. (2.24) becomes

$$\begin{aligned} &V(0)=d\Delta r/2 \\ &V(i)=r_i\Delta r \qquad \text{for } 0<i<M \\ &V(M)=r_M(1+f)\Delta r/2 \\ &V(i)=r_i f\Delta r \qquad \text{for } M<i<N \\ &V(N)=r_N f\Delta r/2. \end{aligned} \tag{2.27}$$

The matrix elements of $\mathbf{W}$ are again given as in Eq. (2.22) for $r_i<r_M$. For $r_i>r_M$ they can be obtained from the elements of Eq. (2.22) by dividing by f^2. The Mth row is determined by the conservation of probability [Eq. (26)] with the $V(i)$'s of Eq. (2.27). One finds

$$\begin{aligned} &W_{M,M-1}=[2/(1+f)](D/\Delta r^2) \\ &W_{M,M}=-(2/f)(D/\Delta r^2) \\ &W_{M,M+1}=[2/(1+f)f](D/\Delta r^2). \end{aligned} \tag{2.28}$$

D. The Matrix Solution

One now needs the matrix elements of $\mathfrak{K}(r)^x\rho$. These are obtained utilizing Eqs. (2.2)–(2.4). One

finds that

$$\mathcal{H}^x(S,T_0)=\begin{array}{c} \begin{matrix} SS & ST_0 & T_0S & T_0T_0 \end{matrix} \\ \begin{pmatrix} 0 & -Q & Q & 0 \\ -Q & 2J(r) & 0 & Q \\ Q & 0 & -2J(r) & -Q \\ 0 & Q & -Q & 0 \end{pmatrix} \end{array} \tag{2.29}$$

for the subspace defined by the S and T_0 levels. In the high-field approximation this subspace does not couple to the remainder of the 16×16 dimensional space needed for a complete representation of $\mathcal{H}^x$. Furthermore, in this approximation, $[\mathcal{H}^x\rho]_{T_+T_+}=[\mathcal{H}^x\rho]_{T_-T_-}=0$, so the $T_\pm$ states cannot contribute to the polarization process. Note that in Eq. (2.29)

$$2Q\equiv(g_a-g_b)\beta_e\hbar^{-1}B_0 + (\sum_j{}^a A_j{}^a M_j{}^a - \sum_k{}^b A_k{}^b M_k{}^b) \tag{2.30}$$

so $2Q$ is the difference in ESR resonant frequencies between radicals a and b (when $J=0$). Actually Eqs. (2.29) and (2.30) imply a particular configuration of nuclear spin states in the two radicals, but this is sufficiently general for considering the interaction of an arbitrary radical pair.

One easily finds that by transforming the matrix of Eq. (2.29) to a representation of

$$\rho\pm\equiv(1/\sqrt{2})(\rho_{S,S}\pm\rho_{T_0,T_0})$$

instead of $\rho_{S,S}$, $\rho_{T,T}$ etc. that $[\mathcal{H}^x\rho]_{+,+}=0$, which just expresses the conservation of spin in the reduced four-dimensional subspace. This can (in the absence of spin-selective chemical reactions, which destroy radicals, see Sec. E) be used to convert the needed subspace to just three dimensions.

The complete solution given by Eq. (2.10) now becomes a matrix equation[3]:

$$[s\mathbf{1}-\mathbf{W}'+i\boldsymbol{\Omega}]\hat{\boldsymbol{\varrho}}(s)=\hat{\boldsymbol{\varrho}}(0) \tag{2.31}$$

such that the vector space in which $\hat{\boldsymbol{\varrho}}(s)$ is defined is the $4(N+1)$ dimensional space formed from the product of the four-dimensional spin space [of Eq. (2.29)] and the $N+1$ dimensional space of Eq. (2.22). The conservation of total probability ($\mathcal{P}$) in this space is given by

$$\mathcal{P}(s)=\int_0^\infty r[\hat{\rho}_{S,S}(r,s)+\hat{\rho}_{T_0,T_0}(r,s)]dr = \sum_{i=0}^{N} V(i)[\hat{\rho}_{S,S}(i,s)+\hat{\rho}_{T_0T_0}(i,s)]=1/s. \tag{2.32}$$

That is, we normalize to unity just in terms of S and T_0 states neglecting the unimportant $T_\pm$ states. The $\boldsymbol{\Omega}$ in Eq. (2.31) is block diagonal, where each block is given by Eq. (2.29) for the particular value of r. The $\mathbf{W}'$ in Eq. (2.31) is just the $\mathbf{W}$ matrix of Eq. (2.22) [as modified according to Eq. (2.28) and the associated discussion], but with each element replaced by the product of that element and a 4×4 unit matrix, since $D\Gamma_r$ is independent of spin.[10]

One solves Eq. (2.31)[16a] for the elements of $\hat{\boldsymbol{\varrho}}(s)$ or $\hat{\rho}(i,s)$ and then the polarization is given, from Eq. (2.17) by

$$P_a{}^\infty=-2\lim_{s\to0} s\sum_{i=0}^{N} V(i)\,\mathrm{Re}[\hat{\rho}_{ST_0}(i,s)]. \tag{2.33}$$

The vector $\hat{\boldsymbol{\varrho}}(0)$ in Eq. (2.31) consists of the initial conditions. One can anticipate a variety of initial conditions (cf. Sec. II.B), but since Eq. (2.21) is linear and homogeneous in $\rho(r,t)$, then one is free to superpose solutions for the simplest forms of initial conditions to obtain solutions for more complex initial conditions. We have only had to consider the case of pure singlet at $r_0=d$, for which $\hat{\rho}_{S,S}(i,t=0)=\delta_{i,0}/V(0)$. The case of pure T_0 at $r_0=d$ may easily be shown to give values of $P_a(t)$ exactly opposite to that obtained from the pure S initial condition. One first rewrites Eq. (2.29) in a coupled basis set as[16b]:

$$[\mathcal{H}^x\rho]_{S,T_0}=\sqrt{2}^{-1}\begin{pmatrix} 0 & J & 0 \\ J & 0 & -Q \\ 0 & -Q & 0 \end{pmatrix} \times \begin{pmatrix} (\rho_{S,T_0}+\rho_{T_0,S}) \\ (\rho_{S,T_0}-\rho_{T_0,S}) \\ (\rho_S-\rho_{T_0}) \end{pmatrix}. \tag{2.34}$$

The term in $(\rho_S+\rho_T)$ is uncoupled as already noted. The initial condition $\rho(0)$ in the same basis as Eq. (2.34) is for pure triplets, thus seen to be just minus that for pure singlets [note $\rho_{S,T}(i,t=0)=0$]. The superposition property of the solution to Eq. (2.1), then means that $P_a(t)$ given by Eq. (2.15a) (recalling $T_\pm$ states do not contribute) only changes in sign. Any mixture of S and T_0 initial states then follows from the superposition. Thus initial random distribution of singlets and triplets cannot give any polarization. Other kinds of initial conditions are considered when the effects of chemical reaction are discussed.

By similar arguments to that just given, one finds from the form of Eqs. (2.31) and (2.34), that the effect of letting $Q\to-Q$ is equivalent to changing the sign of the polarization provided the initial condition is just some admixture of singlet and triplet [with no initial polarization, i.e., $\rho_{S,T}(i,t=0)=0$]. [Similar conclusions may be obtained from Eqs. (2.15) and (2.30) for the definition of Q.] The effect of changing $J\to-J$ is also seen, from Eq. (2.34), to result in a

reversal in sign of the polarization [provided $\rho_{S,T}(i, t=0)=0$].

E. Polarization Effects of a Selective Chemical Reaction

One conclusion of Sec. II.D was that no polarization could be created unless there was an excess of singlets or triplets. When two independently produced radicals happen to collide, then there will be equal probabilities of forming a singlet or each of the triplet states and as a result no polarization. This situation however is changed if the radicals can react via a selective chemical reaction, i.e., the probability for a reaction is higher for singlets than for triplets (or vice versa). Such a selective reaction will have the effect of eliminating some singlets at the first encounter leaving a net triplet character. The situation is now similar to that we have previously considered. Therefore the polarization process may now begin. We shall follow the usual approach, by assuming that the probability for reaction is proportional to the singlet character of the colliding radicals and also that the radicals have to be within a certain distance to react. [The latter assumption is essentially equivalent to a sphere of influence concept.[17]] Thus we define a "first-order chemical rate constant" $k(r)$ that gives the probability of the radical pair reacting per unit time as a function of the interradical separation r. It is necessary to introduce this "rate constant" into an augmented $\mathbf{W}'$-matrix, to allow for disappearance of singlet (or triplet) at the first encounter as well as *all* subsequent radical-pair encounters. One may use a variety of forms for the functional dependence of $k(r)$ on r. We have utilized the simple form

$$k(r_i)=k\delta_{i,0} \tag{2.35}$$

so the "sphere of influence" is just d to $d+\Delta r$.

We then may take as our initial condition, the instant when the radical pair first approaches to the minimum separation d, since no polarization can previously have been built up for random-initial singlet and triplet character. Thus, our solutions based on Eq. (2.33) just give the total polarization developed per radical-pair "collision," where by a single collision we include the first encounter and *all* re-encounters of the radical pair before they finally diffuse away. This polarization also includes the effect of the chemical reaction in depleting the total number of radicals.

The augmented $\mathbf{W}'$ matrix [cf. Eq. (2.31)] that properly includes the effects just described of the chemical reaction is given by letting

$$\mathbf{W}'(k)=\mathbf{W}'(k=0)-k\begin{pmatrix}1 & & & & & \\ & \tfrac{1}{2} & & & & \\ & & \tfrac{1}{2} & & & \\ & & & 0 & & \\ & & & & 0 & \\ & & & & & \cdot \\ & & & & & & \cdot \\ & & & & & & & \cdot\end{pmatrix}, \tag{2.36}$$

i.e., decay of radical only from d to $d+\Delta r$ and only that of pure singlet character. The associated off-diagonal density-matrix elements $\rho_{ST_0}(d)$ and $\rho_{T_0S}(d)$ must also decay by a Heisenberg uncertainty in life-time effect given as the mean of the decay rate of S and T_0 states,[2e,18] or just $\frac{1}{2}k$.

When Eq. (2.36) is utilized, then the total probability $\mathcal{P}(t)$ [or $\mathcal{P}(s)$ its Laplace transform] given by Eq. (2.32) is no longer unity, reflecting the loss of radical due to the chemical reaction. We define the recombination probability per "collision" as

$$\mathcal{F}=1-\mathcal{P}, \tag{2.37}$$

where

$$\mathcal{P}\equiv\lim_{t\to\infty}\mathcal{P}(t).$$

It is therefore useful to define a normalized polarization P_a as

$$\bar{P}_a(t)=-2\,\mathrm{Tr}[\rho(t)S_{az}]/\mathrm{Tr}\rho(t)=P_a(t)/\mathcal{P}(t). \tag{2.38}$$

$\bar{P}_a(t)$ gives the correct polarization for the radicals that survive the "collision." (However, it will be shown in Sec. IV that the quantity most directly related to experimental results is $P_a^{\infty}/\mathcal{F}$.)

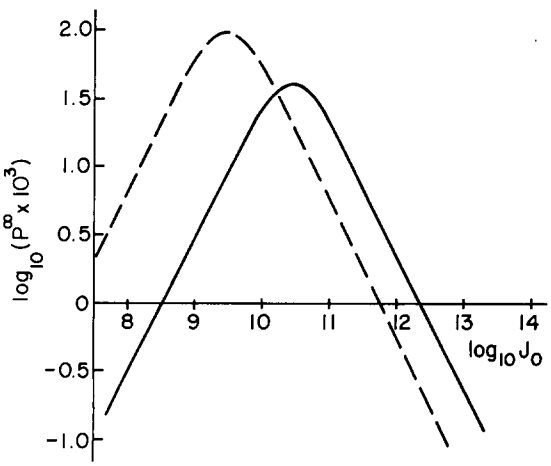

FIG. 1. Polarization P_a^{∞} as a function of J_0 for the contact exchange model. Solid curve: $D=10^{-5}$ cm²/sec and dashed curve: $D=10^{-6}$ cm²/sec. Other parameters used are $Q=0.5\times10^8$ sec^{-1}, $d=4$ Å, $\Delta r=1$ Å. Graph gives $\log_{10}(P_a^{\infty}\times10^3)$ vs $\log_{10}J_0$. Sign of P_a^{∞} determined as in Table II. This graph scales by replacing the abscissa variable $\log_{10}(J_0)$ by $\log_{10}[10^{\epsilon}J_0d^2/16D]$ and by using $Qd^2/16D=0.5\times10^{(8-\epsilon)}$ where $\epsilon=11$ and 10 for the solid and dashed curves, respectively, and $\Delta r/d=1/4$.

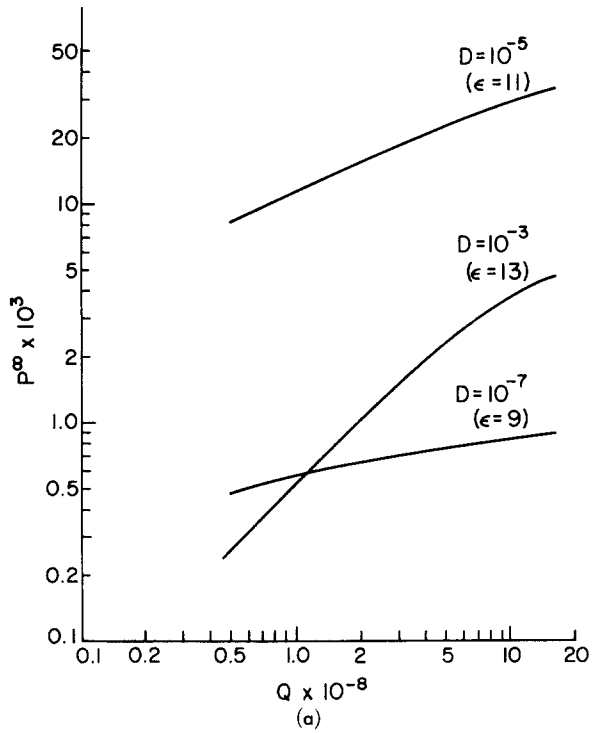

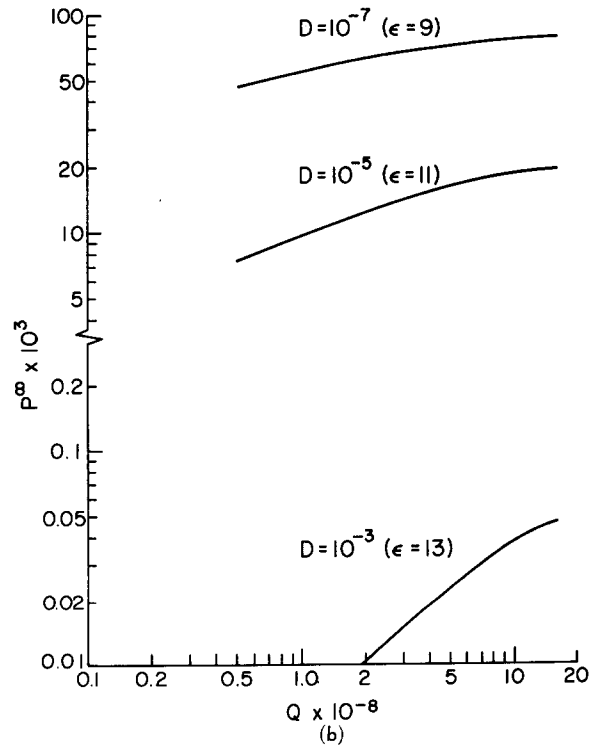

FIG. 2(a). P_a^∞ as a function of Q for the contact exchange model. Separate curves are for $D=10^{-3}$, 10^{-5}, 10^{-7} cm²/sec. Other parameters used are $J_0=10^{12}$ sec^{-1}, $d=4$ Å, $\Delta r=0.25$ Å. Sign of P_a^∞ determined as in Table II. This graph scales by replacing the abscissa variable $Q\times10^{-8}$ by $(Qd^2/16D)\times10^{\epsilon-8}$, and each curve corresponds to a particular value of $J_0d^2/16D=1\times10^{(12-\epsilon)}$ for A and $1\times10^{(10-\epsilon)}$ for B. The values of ϵ are shown. Also $\Delta r/d=1/16$. (b) Same as (a), but $J_0=10^{10}$ sec^{-1}.

III. RESULTS

The Eqs. (2.31) and (2.33) are very conveniently solved by the use of Gaussian elimination of banded matrices on a 360/65 IBM computer, with only about a second of running time for each calculation.[19,20] We found that the limit $s\to0$ needed for Eq. (2.33) was always reached for $s\lesssim10^{-8}D/(\Delta r^2)$. The actual convergence with s can be seen in Table I.

In our computations, we have employed as the form of $J(r)$

$$J(r)=J_0\exp[-\lambda(r-d)] \quad \text{for } r\geq d \tag{3.1a}$$

or

$$J(r_j)=J_0\exp[-j\lambda\Delta r] \qquad \text{for } j=0,1\cdots M. \tag{3.1b}$$

[In discussing our results, it is convenient to define a distance r_{ex} for which $J(r+r_{ex})=10^{-5}J(r)$, or $r_{ex}=\lambda^{-1}5\ln10$.] In the limit as λ gets very large, Eq. (3.1b) is just a simple "contact exchange" model:

$$J(r_j)=J_0\delta_{j,0}. \tag{3.1c}$$

More precisely, this contact exchange model is one in which the molecules are either in or out of the region where $J_0\neq0$. It does not allow for the molecules to take any diffusive steps and remain in the region where $J_0\neq0$.

We have solved Eqs. (2.31) followed by Laplace inversion to obtain $P_a(t)$ [cf. Eq. (2.15)] as a function of time for several cases. One finds that the polarizations have fully developed in 10^{-8} sec for $D=10^{-5}$ cm²/sec, 10^{-7} sec for $D=10^{-6}$ cm²/sec, (and $r_N\sim100$–200 Å), and in general, the time of development of polarization is inversely proportional to D. (These time evaluation results are fully consistent with our findings on convergence as $s\to0$ cf. Table I.) This justifies our neglect of T_1 processes during the collision. They are explicitly included in the rate analysis of Sec. IV.

We have found that satisfactorily convergent solutions (cf. Table I) are obtained [with Eq. (3.1b)] when Δr is chosen so that[20] $J(r_i)/J(r_i+\Delta r)=e^{\lambda\Delta r}\lesssim5$, and then M is taken so that $J(r_M)\approx0$ while $r_N\sim100$–200 Å for $D\geq10^{-4}$ sec with $f\sim10$–20.[21a] (However, for $D=10^{-3}$ cm²/sec and smaller $Q\sim10^8$ sec^{-1}, very large values $r_N\sim900$ Å are needed to guarantee convergence, although most results below are given for $r_N\sim200$ Å, since new collisions and reactions should occur at such distances in moderate concentrations. Note that a study of P_a^∞ vs r_N can show the role played by re-encounters in both building up new polarization and in destroying previously built-up polarization.)

Scaling of Results. One finds that the system of Eqs. (2.8)–(2.11), (2.19), (2.35), and (3.1) permit a scaling by introducing the dimensionless variables $x=(r/d)-1$ and $\tau=Dt/d^2$, while solving for $\Phi(x,\tau)\equiv d^{-1}\hat{\rho}(r,t)$ for the limit $\tau\to\infty$.[21b] One then has from Eqs. (2.13), (2.14),

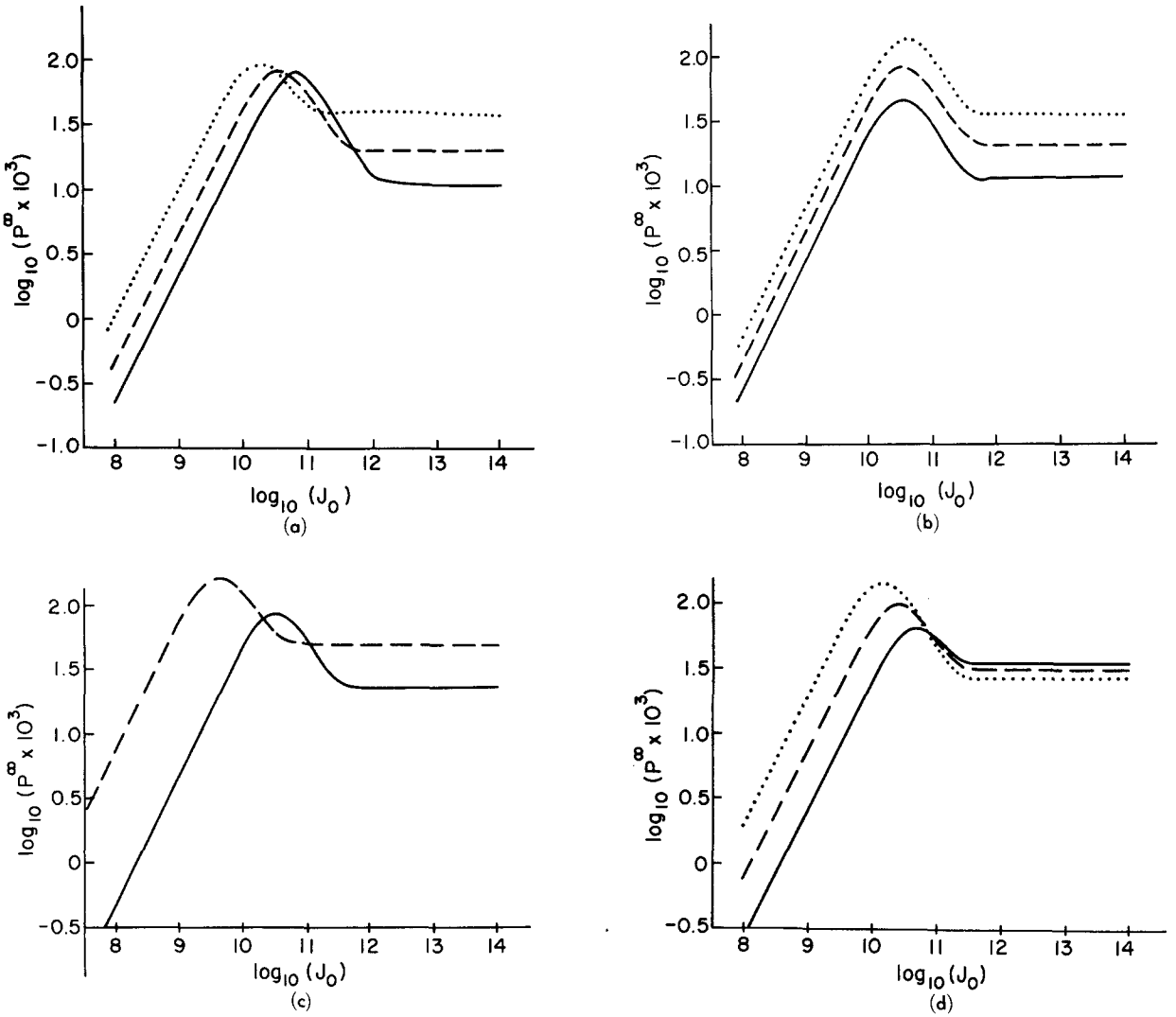

FIG. 3(a). P_a^∞ as a function of J_0 for initial singlet (or triplet) state. Solid curve: $r_{ex}=2$ Å, dashed curve: $r_{ex}=4$ Å, dotted curve: 8 Å. Other parameters used are $D=10^{-5}$ cm²/sec, $Q=2\times10^8$ sec^{-1}, $d=4$ Å. Sign of P_a^∞ determined as in Table II. This graph scales by replacing the abscissa variable $\log_{10}(J_0)$ by $\log_{10}[10^{11}J_0d^2/16D]$ and by using $r_{ex}/d=1/2$, 1, and 2, respectively, and $Qd^2/16D=2\times10^{-3}$. (b). P_a^∞ as a function of J_0 for initial singlet (or triplet) state. Solid curve: $Q=0.5\times10^8$ sec^{-1}, dashed curve: $Q=2\times10^8$ sec^{-1}, dotted curve: $Q=8\times10^8$ sec^{-1}. Other parameters used are $D=10^{-5}$ cm²/sec, $r_{ex}=4$ Å, $d=4$ Å. Sign of P_a^∞ determined as in Table II. This graph scales by replacing the abscissa variable $\log_{10}(J_0)$ by $\log_{10}[10^{11}J_0d^2/16D]$ and by using $Qd^2/16D=1\times10^{-11}Q$ and $r_{ex}/d=1$. (c). P_a^∞ as a function of J_0 for initial singlet (or triplet) state. Solid curve: $D=10^{-5}$ cm²/sec; dashed curve: $D=10^{-6}$ cm²/sec. Other parameters used are $Q=2.0\times10^8$ sec^{-1}, $r_{ex}=4$ Å, $d=4$ Å. Sign of P_a^∞ determined as in Table II. (d). P_a^∞ as a function of J_0 for initial singlet (or triplet) state. Solid curve: $d=2$ Å, dashed curve: $d=4$ Å, dotted curve: $d=8$ Å. Other parameters used are $Q=4\times10^8$ sec^{-1}, $r_{ex}=4$ Å, $D=10^{-5}$ cm²/sec. Sign of P_a^∞ determined as in Table II.

and (2.16) that the polarization P_a^∞ may be written as

$$P_a^\infty(J_0, Q, r_{ex}, D, d, k) \rightarrow P_a^\infty(J_0d^2/D, Qd^2/D, r_{ex}/d, kd^2/D),$$

i.e., the apparent dependence of P_a^∞ on the six variables J_0, r_{ex}, Q, D, d, and k may be reduced to a dependence on just four dimensionless variables J_0d^2/D, Qd^2/D, r_{ex}/d, and kd^2/D. Equivalent comments apply to $\mathcal{P}$ and $\mathcal{F}$. (In the contact exchange model, r_{ex}/d should be replaced by the radial extent of $J_0\neq0$ in units of d.) We show results with respect to the regular dimensional variables for physical clarity but we indicate how they may be scaled based on the dimensionless variables.

A. Contact Exchange Model

The results for $J(r_j)$ given by Eq. (3.1c) are shown in Figs. 1 and 2. In Fig. 1, the functional dependence of P_a^∞ on J_0 is given for several cases. One can fit the curves shown (as well as many other results we have obtained) to the functional form (for $Q<J_0$)

$$P_a^\infty=f(Q, D)(2J_0\tau_1/[1+(2J_0\tau_1)^2]), \quad (3.2)$$

where τ_1 may be interpreted as the lifetime of a bi-

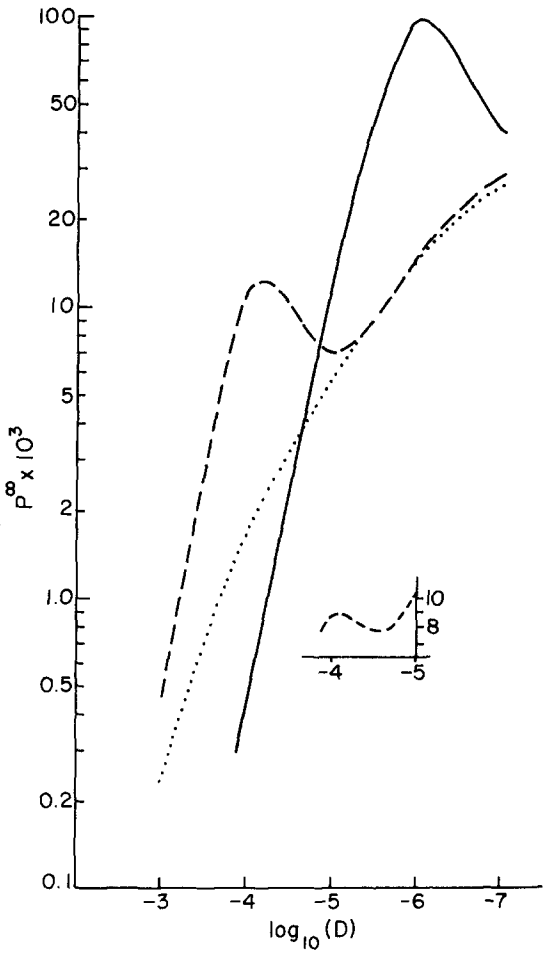

FIG. 4. P_a^{∞} as a function of D for initial singlet (or triplet) state. Solid curve: $J_0=10^{10}$ sec^{-1}, dashed curve: $J_0=10^{12}$ sec^{-1}, dotted curve: $J_0=10^{14}$ sec^{-1}. Other parameters used are $Q=0.5\times 10^8$ sec^{-1}, $r_{ex}=2$ Å, $d=4$ Å. The small insert shows the shape correction to the $J_0=10^{12}$ sec^{-1} curve if $r_{ex}=4$ Å is used. Sign of P_a^{∞} determined as in Table II.

molecular encounter and is found to be well approximated by [cf. Eq. (2.27)]

$$\tau_1 \cong V(0)/D. \tag{3.3}$$

This result for τ_1 may be compared with the usual Brownian diffusion result of $\tau_1^{-1} \cong 4\pi Dd/\Delta V$, where ΔV is the "reaction volume,"[22-24] to show that ΔV is just the annular volume of the "contact region" $4\pi dV(0)$ (which is valid for $\Delta r/2d \ll 1$). The J dependence of Eq. (3.2) is essentially that found for equivalent models of Heisenberg spin exchange,[24,25] although the dependence on D is modified by the coefficient $f(Q, D)$ [which by scaling, may be written as $f(Qd^2/D)$]. The Q dependence of $f(Q, D)$ is strongly dependent on the value of D, as may be seen from Fig. 2. One finds for $Q \sim 10^{-8}$ sec^{-1} that $f(Q,\ 10^{-3}) \propto Q$, $f(Q,\ 10^{-5}) \propto Q^{0.45}$, while $f(Q,\ 10^{-7}) \propto Q^{0.2}$. (However, if $r_N \sim 900$ Å instead of $r_N \sim 200$ A is used, then $f(Q,\ 10^{-3}) \propto Q^{0.48}$.) These results for $f(Q, D)$ are independent of J. The composite of the features in Figs. 1 and 2 has not been adequately predicted by the earlier simplified models.

B. Polarizations in the Absence of Chemical Reactions

Our results on polarizations in the absence of chemical reactions are shown in Figs. 3–5 and in Table II. These are the results for $J(r_i)$ given by Eq. (3.1b). One sees by comparing Figs. 3(a) and 1, that for small J_0 values (dependent on the value of D), all the curves of Fig. 3(a) show identical J dependence as the simple contact-exchange model and with very similar values of P_a^{∞}. But for $J_0 > J_0(\max)$ [where $J_0(\max)$ is the value of J_0 corresponding to a maximum in P_a^{∞}] the polarization P_a^{∞} first decreases, but then levels off to a value virtually independent of J_0, i.e., $P_a^{\infty}(\text{asympt})$. One finds that this asymptotic value is dependent on r_{ex}, the larger the value of r_{ex}, the greater is $P_a^{\infty}(\text{asympt})$ as one would anticipate on simple physical grounds. This important feature is distinctly different from the contact exchange model of Fig. 1 and has the important consequence of permitting significant polarizations to develop even while J_0 may be very large (i.e., $>10^{12}$ sec^{-1}). There is a tendency for $P_a^{\infty}(\text{asympt})$ to depend linearly on r_{ex} [cf. Table II and Fig. 3(a)]. Figure 3(b) shows that $P_a^{\infty}(\text{asympt})$ does depend significantly on Q, i.e., a higher Q value gives a higher $P_a^{\infty}(\text{asympt})$. Figure 3(c) shows a typical effect of D on the maximum in P_a^{∞} as a function of J_0. For $Q \lesssim 10^8$ sec^{-1}, $J_0(\max)$ is approximately proportional to D (as in the "contact exchange" model), but for higher Q values, this is no

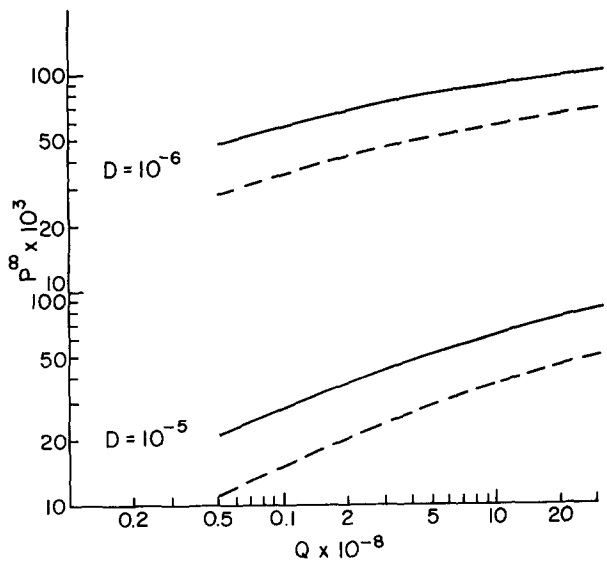

FIG. 5. P_a^{∞} as a function of Q for initial singlet (or triplet) state. Solid lines: $r_{ex}=8$ Å, dashed lines $r_{ex}=4$ Å. Values for $D=10^{-5}$ and 10^{-6} cm^2/sec are given. Other parameters used are $J_0=10^{13}$ sec^{-1} and $d=4$ Å. Sign of P_a^{∞} determined as in Table II. Scaling is according to Eq. (3.4b) and is asymptotic in $J_0d^2/16D$.

TABLE I. Convergence of polarization calculations. $P_a^{\infty}\times10^3$.[a]

Parameter varied s' [b]	10^{-1}/2.4	10^{-2}/17.6	10^{-3}/38.1	10^{-4}/38.8	$\leq10^{-5}$/38.5
Δr, Å[c]	1.0/11.9	0.75/11.3	0.5/11.2	0.25/11.2	
Δr, Å[d]	1.0/21.3	0.75/20.4	0.5/20.3	0.25/20.3	
Δr, Å[e]	1.0/35.2	0.75/34.2	0.5/33.4	0.25/34.2	
r_N, Å[c]	42/6.5	72/10.6	112/11.7	212/11.2	
r_N, Å[d]	42/21.6	72/21.6	112/20.8	212/20.3	
r_N, Å[e]	42/38.4	72/36.1	112/35.1	212/34.2	

[a] P_a^{∞} values are to the right of values of parameters varied. Calculations are for no chemical reaction and singlet initial case. Values of the other parameters used are $D=10^{-5}$ cm²/sec, and $d=4$ Å, $J_0=10^{13}$ sec^{-1}, $r_{ex}=4$ Å, except as noted otherwise.

[b] $s'\equiv s\Delta r^2/D$, $J=10^{14}$ sec^{-1}, $r_{ex}=8$ Å, $Q=2\times10^{-8}$ sec^{-1}.

[c] $Q=0.5\times10^{8}$ sec^{-1}.

[d] $Q=2.0\times10^{8}$ sec^{-1}.

[e] $Q=8.0\times10^{8}$ sec^{-1}.

TABLE II. Asymptotic values of polarizations for large J_0.[a,b,h]

		$r_{ex}=2$ Å[c]		$r_{ex}=4$ Å[d]		$r_{ex}=8$ Å[e]	
$Q\times10^{-8}$ sec^{-1}	D cm²/sec	$P_a^{\infty}\times10^3$ [f]	$\mathcal{P}_g$	$P_a^{\infty}\times10^3$ [f]	$\mathcal{P}_g$	$P_a^{\infty}\times10^3$ [f]	$\mathcal{P}_g$
0.5	10^{-4}	1.68	0.499	3.35	0.499	6.79	0.499
1		2.69	0.497	5.36	0.497	10.7	0.496
2		3.73	0.492	7.42	0.492	14.5	0.492
4		5.12	0.487	10.1	0.487	19.6	0.487
8		7.02	0.480	13.8	0.480	26.3	0.481
16		9.51	0.470	18.5	0.471	34.6	0.473
32		12.7	0.456	24.5	0.459	44.5	0.463
0.5	10^{-5}	5.67	0.484	11.2	0.484	21.6	0.485
1		7.75	0.476	15.2	0.477	28.7	0.478
2		10.5	0.465	20.3	0.466	37.6	0.469
4		13.9	0.450	26.7	0.453	47.9	0.458
8		18.0	0.431	34.2	0.436	59.2	0.446
16		22.5	0.407	42.2	0.416	71.2	0.432
32		27.1	0.379	49.8	0.392	84.0	0.417
0.5	10^{-6}	14.9	0.446	28.1	0.451	48.5	0.458
1		19.0	0.426	35.4	0.434	58.4	0.447
2		23.2	0.403	42.6	0.415	68.2	0.435
4		27.6	0.377	48.7	0.395	78.6	0.424
8		32.8	0.349	55.6	0.375	88.5	0.413
16		37.9	0.319	64.5	0.356	96.6	0.402
32		42.0	0.289	70.7	0.337	104.0	0.392

[a] $J_0=10^{13}$ sec^{-1} was utilized except for $D=10^{-4}$ cm²/sec, where $J_0=10^{14}$ sec^{-1} was used.

[b] The signs of the polarization are determined as follows. i) No chemical reaction: $\mathrm{Sign}[P_a^{\infty}]=-[\mathrm{Sign}Q][\mathrm{Sign}J]\{\mathrm{Sign}[\rho_{SS}(t=0)-\rho_{TT}(t=0)]\}$; ii) spin-selective chemical reaction (reaction of S states): $\mathrm{Sign}[P_a^{\infty}]=[\mathrm{Sign}Q][\mathrm{Sign}J]$.

[c] Values of $d=4$ Å, $\Delta r=0.25$ Å, $M=32$, $N=72$, $r_N=212$ Å utilized.

[d] Values of $d=4$ Å, $\Delta r=0.25$ Å, $M=32$, $N=72$, $r_N=212$ Å utilized.

[e] Values of $d=4$ Å, $\Delta r=0.5$ Å, $M=32$, $N=72$, $r_N=220$ Å utilized.

[f] The results are given for $P_a^{\infty}\times10^3$ in the no chemical reaction case and for $(P_a^{\infty}/\mathcal{F})\times10^3$ in the spin-selective reaction case (with random initial condition). For no chemical reaction, multiply table entry by $|\rho_{SS}(t=0)-\rho_{T_0T_0}(t=0)|$.

[g] Survival probability for R.I. condition in the presence of a spin-selective chemical reaction with $k=10^{15}$ sec^{-1}, i.e., $k\Delta r^2/D\gg1$. Note that $\tilde{P}_a^{\infty}$ and $\mathcal{P}$ scale for different values of $k\Delta r^2/D$ as shown in Fig. 7.

[h] The results of this table scale according to Eq. (3.4b); thus if $Q=22\times10^8$, $r_{ex}=4$ Å and $d=2$ Å, one obtains the same polarization as for $Q=5.5\times10^8$ sec^{-1}, $r_{ex}=8$ Å and $d=4$ Å, which may be interpolated from the table.

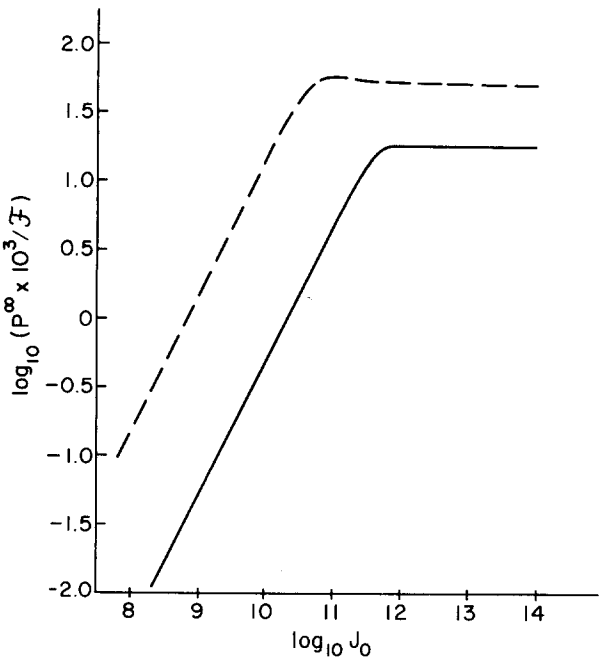

FIG. 6. $P_a^\infty/\mathcal{F}$ as a function of J_0 for spin-selective chemical reactions. Curves shown for random initial (R.I.) condition, with solid curve: $D=10^{-5}$ cm²/sec and dashed curve: $D=10^{-6}$ cm² /sec. Other parameters used are $r_{ex}=4$ Å, $Q=10^8$ sec^{-1}, $d=4$ Å, $k\Delta r^2/D\gg 1$. Sign of P_a^∞ determined as in Table II. This graph scales by replacing the abscissa variable $\log_{10}(J_0)$ by $\log_{10}[10^\epsilon J_0 d^2/16D]$ and by using $Qd^2/16D=1\times 10^{(8-\epsilon)}$ where $\epsilon=11$ and 10 for the solid and dashed curves, respectively. Also $r_{ex}/d=1$.

longer strictly true [cf. Fig. 3(c)]. The dependence of P_a^∞ on the contact distance d is illustrated in Fig. 3(d) (again given as a function of J_0). For $J_0<J_0(\max)$ there are significant differences for the different d values, with P_a^∞ increasing as d increases. However, the P_a^∞(asympt) (for $J_0>10^{12}$ sec^{-1}) are quite similar for the different d values although they do increase slightly with decreasing d. This latter variation [$\sim 10\%$ in Fig. 3(d)] is increased for larger Q values, but decreases for smaller Q values. In all other graphs and our tables, we have used a single value of $d=4$ Å. The composite of the parts of Fig. 3 may be summarized by the simple relations (based on dimensionless variables)

$$P_a^\infty \cong h(Qd^2/D)(J_0 d^2/D)(r_{ex}/d) \qquad \text{for } J<J_0(\max) \tag{3.4a}$$

and

$$P_a^\infty(\text{asympt}) = \bar{g}(Qd^2/D,\ r_{ex}/d) \cong g(Qd^2/D)(r_{ex}/d) \tag{3.4b}$$

where f, g, and h are very similar functions of Qd^2/D. Also if a τ_1 is defined (by analogy with the contact exchange model) as $2J_0(\max)\tau_1=1$, then we find:

$$\tau_1 \cong (d^2/D)(\lambda d)^{-1} \cong 0.1(d^2/D)(r_{ex}/d) \tag{3.4c}$$

(neglecting effects of Q).

Figure 4 shows P_a^∞ as a function of D for various values of J_0. One finds that P_a^∞ goes through a local maximum, the position of which is determined by J_0. For $J_0=10^{12}$ sec^{-1} this maximum lies in the normal diffusion region, while for $J_0=10^{10}$ sec^{-1} or $J_0=10^{14}$ sec^{-1} this local maximum will lie in the very fast or very slow diffusion limit, respectively. The existence of this local maximum is closely related to the maximum in P_a^∞ versus J_0 shown in Fig. 3. The effect of changing Q is merely to shift the x axis. The effect of changing r_{ex} is shown in the small insert. A larger r_{ex} gives a less pronounced local maximum. This suggests that if experiments could be performed that yield P_a^∞ as a

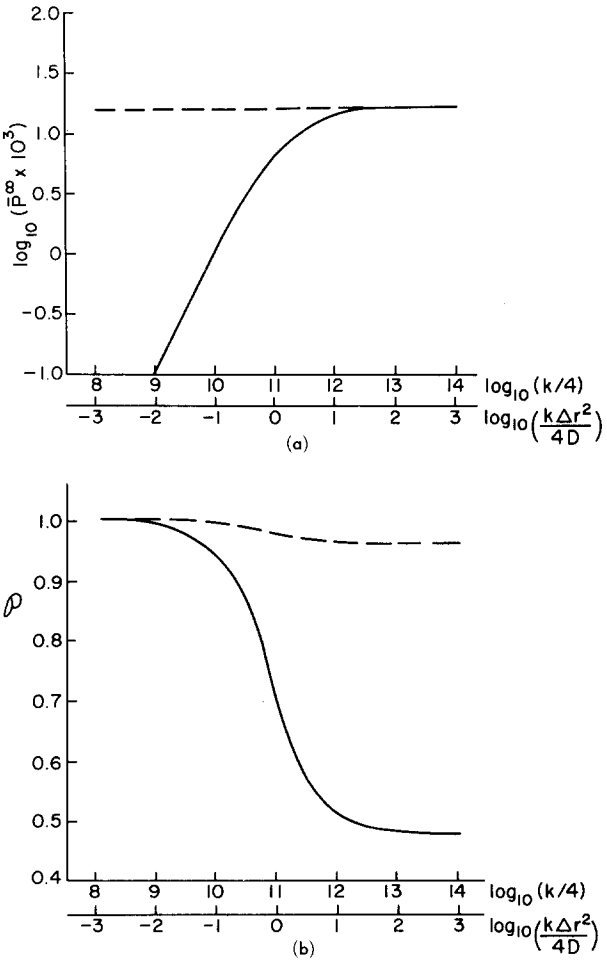

FIG. 7. Graphs of (a) $\bar{P}_a^\infty$ and (b) $\mathcal{P}$ as a function of k for spin-selective chemical reactions. The solid lines are for random initial (R.I.) and the dashed for triplet initial (T.I.) conditions. Other parameters used are $J_0=10^{13}$ sec^{-1}, $r_{ex}=4$ Å, $Q=1\times 10^8$ sec^{-1}, $d=4$ Å, $\Delta r=1$ Å. Sign of $\bar{P}_a^\infty$ determined as in Table II.

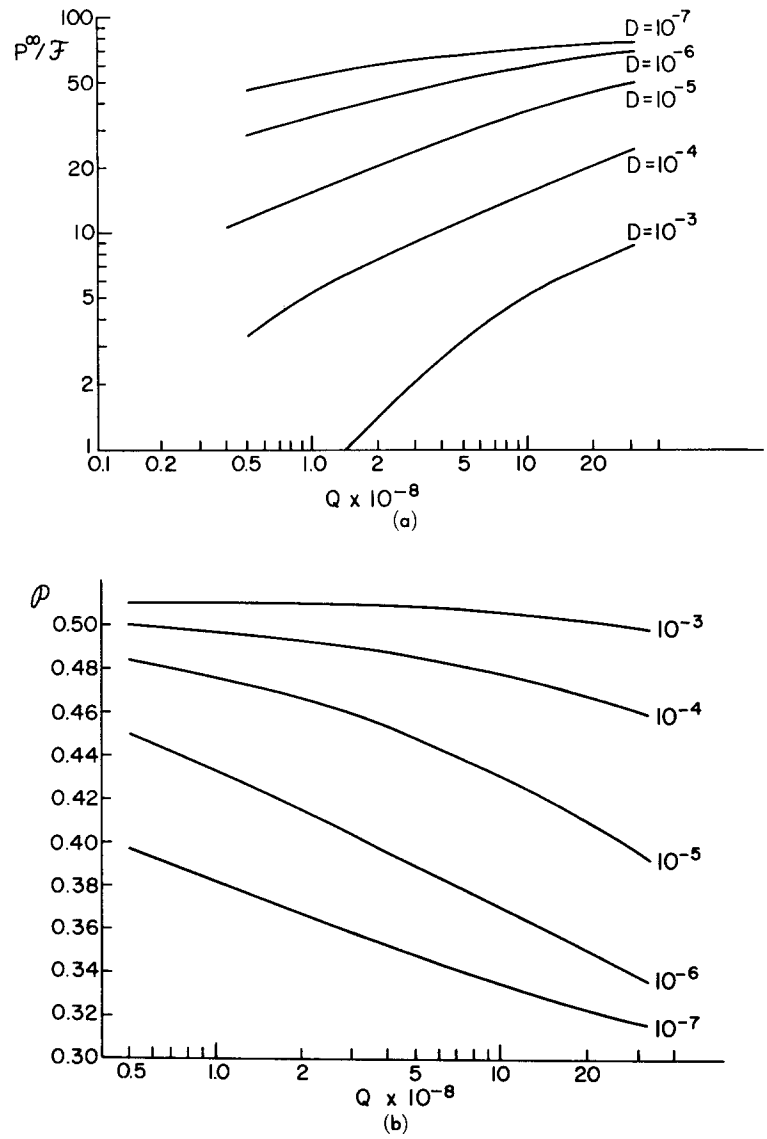

FIG. 8. Graphs of (a) $P_a^\infty/\mathcal{F}$ in units of 10^{-3} and (b) $\mathcal{P}=1-\mathcal{F}$ as a function of Q for spin-selective chemical reactions. Curves shown for random initial (R.I.) condition and for values of D of 10^{-3} and 10^{-4} cm²/sec with $J_0=10^{14}$ sec^{-1}, and values of 10^{-5}, 10^{-6}, and 10^{-7} cm²/sec with $J_0=10^{13}$ sec^{-1}. Other parameters used are $r_{ex}=4$ Å, $d=4$ Å, $k\Delta r^2/D\gg 1$. Sign of $\bar{P}_a^\infty/\mathcal{F}$ determined as in Table II. Scaling is according to Eq. (3.4b) and is asymptotic in $J_0d^2/16D$.

function of D, it might be possible to determine something about the properties of $J(r)$. The dependence of P_a^∞ on Q for different r_{ex} and D is illustrated in Fig. 5. The value of r_{ex} has almost no effect on the functional form of P_a^∞ on Q, as predicted by Eq. (3.4b), and this functional form is very similar to that obtained for the contact exchange model.

We present in Table II a range of values of P_a^∞, which should be useful for the experimenter as well as for comparison with results that may be obtained from more approximate theoretical models. Since it is most likely true that $J_0>10^{12}$ sec^{-1} (and also to avoid excessive tabulation), we present P_a^∞(asympt) in terms of all the other relevant parameters.

C. Polarizations in the Presence of Spin-Selective Chemical Reactions

Some of our results for the case of polarizations in the presence of spin-selective chemical reactions are summarized in Table II and in Figs. 6–8. We consider as initial conditions, either the random (R.I.) case (equal amounts of S and T_0) or pure triplet (T.I.), where only T_0 is included. One finds from Fig. 6 that the functional dependence of $P_a^\infty/\mathcal{F}\approx\bar{P}_a^\infty$ upon J_0 is somewhat similar in form to that shown in Fig. 3 for no chemical reaction. However, the maximum in $P_a^\infty/\mathcal{F}$ has virtually disappeared compared to the asymptotic value of $P_a^\infty/\mathcal{F}$. Figure 7 shows typical results for the dependence of P_a^∞ and $\mathcal{P}$ on k [of Eq. (35)]. One finds that for $\Delta r^2k/D\gtrsim 1$ both $\bar{P}_a^\infty$ and $\mathcal{P}$ achieve an asymptotic value independent of k, while $\bar{P}_a^\infty$ is also independent of whether the initial condition is R.I. or T.I. Actually P_a^∞ for T.I. is nearly independent of k, while for R.I. and $\Delta r^2k/D<1$ it drops off very rapidly to negligible values. These results are as expected, since for $\Delta r^2k/D>1$, any radicals in an S_0 state would completely react before diffusing out leaving only triplets, or half the initial number of radicals in the case of

R.I., while for $\Delta r^2k/D<1$ the R.I. condition is not modified sufficiently to generate significant polarization P_a^∞ (cf. Sec. II.E). Note that $\mathfrak{F}=1-\mathcal{P}$ from Fig. 7(b) gives for T.I. the combined probability that a radical pair initially together in a T_0 state will have first been converted to S_0 and then react.

One finds from a comparison of Fig. 8(a) (for R.I. and $\Delta r^2k/D>1$) and Fig. 2 (for the contact exchange model) that the Q dependence of $P_a^\infty/\mathfrak{F}$ is virtually the same as that for P_a^∞ calculated for no reaction and contact exchange. By comparing Fig. 8(a) with Fig. 5 (no reaction, T.I., and the same exchange interaction) one observes that not only is the Q dependence of $P_a^\infty/\mathfrak{F}$ (R.I., with reaction) and P_a^∞ (T.I., no reaction) identical in the two cases, but the actual values of $P_a^\infty/\mathfrak{F}$ are also identical.

We have also examined the k dependence of $P_a^\infty/\mathfrak{F}$ and have found that $P_a^\infty/\mathfrak{F}$ is independent of k for such values of J_0 that P_a^∞ has assumed its asymptotic value. This, of course, means that the functional forms of P_a^∞ and $\mathfrak{F}$ on k are identical. For lower values of J_0 we found that $P_a^\infty/\mathfrak{F}$ has a weak dependence on k, but it is much weaker than that of P_a^∞ [cf. Fig. 7(a)]. For normal diffusion rates (i.e., $D=10^{-4}$–10^{-5} cm^2/sec) and $J_0>10^{10}$ sec^{-1} one can take $P_a^\infty/\mathfrak{F}$ to be independent of k.

One observes from Fig. 8(b), that the fraction of radicals that have reacted ($\mathfrak{F}$) is larger both for smaller values of D and for larger values of Q. This Q dependence is presumably due to radical pair re-encounters. The larger the Q value, the more effective is the S–T_0 mixing. Then the radicals undergoing a second or higher encounter will have developed greater S character for higher Q. Thus one predicts $\mathfrak{F}>0.5$ in the R.I. case. (For the T.I. case, $\mathcal{P}$ is exactly twice that for the R.I. case.) The D dependence in Fig. 8(b) is probably due to the fact that a smaller D value means slower motion, hence more time for the S–T_0 mixing process.

Note that the values in Table II are again for $P_a^\infty/\mathfrak{F}$(asympt) and also for $k\Delta r^2/D>1$. As we have just noted, these values are identical to P_a^∞ for the no reaction case.

D. Conjectures on Interpretation

The dependence of P_a^∞ on Q for different values of D as illustrated in Fig. 2 and 8(a) and detailed in Table II is useful in trying to determine the nature of the polarization process in terms of the simpler models given by earlier workers and recently reviewed by Freed.[3] The $P_a^\infty \propto Q$ dependence for very fast diffusion may be compared to the simple result obtained from polarization due to an initial encounter for the contact exchange model,[3] when, for $J_0 \gg Q$,

$$P_a^\infty \propto (Q/J_0)\{(2J\tau_1)/[1+(2J\tau_1)^2]\}.$$

It is as though there is not sufficient time for S–T_0 mixing via Q when the radicals are apart, and the very small polarizations generated (even from subsequent encounters) will occur essentially as that for the initial encounter. This appears justified by our observation that when r_N is increased from $\sim$200 Å to $\sim$900 Å, so that re-encounters due to radicals which have first separated by very large distances are included, then $P_a^\infty \propto Q^{0.48}$. As the motion slows down, there is then sufficient time for S–T_0 mixing while the radicals are apart thus enhancing the polarization at a subsequent encounter (e.g., the mechanism suggested by Adrian[7] where $P \propto Q^{1/2}$). But, as the motion becomes even slower, one might expect that the S–T_0 mixing becomes optimal for all Q values, so that the polarization becomes almost independent of Q.

The fact that $P_a^\infty \rightarrow P_a^\infty$(asympt) for $J_0>10^{12}$ sec^{-1} may, in part, be rationalized in terms of the fact that the effective region of polarization [which includes the "desirable" range in $J(r)$, i.e., $J(r)<10^{12}$ sec] merely moves out further from r_0, while the inner region [where $J(r)>10^{12}$ sec^{-1}] is probably primarily effective in just cancelling any polarizations via the spin-exchange mechanism,[1c,24] or by the spin-selective chemical reaction.

The fact that $P_a^\infty/\mathfrak{F}$ becomes independent of k for large J_0 can be understood by the following arguments. The chemical reaction acts to eliminate a fraction $\mathfrak{F}(k)$ of singlets. If one assumes that this is the only effect of the chemical process, one may then calculate the polarization as though there were no chemical reaction, but with the initial condition $[\rho_{T_0T_0}(0)-\rho_{SS}(0)]=\mathfrak{F}(k)$. Since P_a^∞ is proportional to $[\rho_{T_0T_0}(0)-\rho_{SS}(0)]$, we see that $P_a^\infty/\mathfrak{F}$ becomes independent of k and equal to P_a^∞ (T.I., no reaction). It is easy to see that this argument is valid even though the total disappearance of singlets also involves subsequent encounters. The assumption that the only effect of the chemical process, represented by k, is to destroy singlets corresponds to neglecting the two matrix elements with value $k/2$ in Eq. (2.36). The effect of these elements is to destroy polarization in the region d to $d+\Delta r$ [cf. Eq. (2.35)]. If $J_0>J_0(\max)$, then the polarization in this region is quenched anyway by spin exchange and the assumption is then valid. For $J_0<J_0(\max)$, one would expect these matrix elements to become important; therefore $P_a^\infty/\mathfrak{F}$ should depend on k, as one in fact finds.

IV. CIDEP INTENSITIES

The polarization results given in Sec. III are for single encounters. These polarizations will, of course, decay to the equilibrium value P_{eq} due to T_1 processes. Also the radicals carrying the polarization may be destroyed due to chemical processes. New radicals may also be formed, for example, due to a light source.

The ESR intensity depends not only on the actual

polarization but also on the number of radicals. To calculate the ESR intensity for a CIDEP experiment, we therefore have to include the actual kinetics of the system. We illustrate the way in which this may be done with some simple examples. These examples will show that the observed CIDEP intensity depends not only on P_a^∞ but also on T_1 and $t_{1/2}$ (the half-life of the radical) in such a way that even if $P_a^\infty<0$ for a given line, this in itself is not sufficient for the line to appear in emission.

The CIDEP intensity at time t $I_a(t)$ may simply be defined as

$$I_a(t)=n_a(t)P_a(t), \tag{4.1}$$

where $n_a(t)$ is the number of radicals of type a. General rate equations may be written for $n_a(t)$ as well as $n_b(t)$:

$$dn_a(t)/dt=k_{0,a}-k_{1,a}n_a(t)-k_2n_a(t)n_b(t)\mathfrak{F} \tag{4.2a}$$

$$dn_b(t)/dt=k_{0,b}-k_{1,b}n_b(t)-k_2n_a(t)n_b(t)\mathfrak{F}. \tag{4.2b}$$

The zero order k_0 terms are the radical source terms due to a light beam, electron beam, etc. The first order reaction may be due to reactive collisions with other radicals or molecules, where we assume for convenience that the latter are in sufficient concentration that their amounts hardly change. The second order reaction is due to radical–radical recombination. The rate constant is most conveniently written as $k_2\mathfrak{F}$, where $k_2n_an_b$ gives the frequency of collisions and $\mathfrak{F}$ gives the probability for recombination per collision, [cf. Eq. (2.37)]. This reaction is taken as being spin selective requiring an S spin state. For convenience in comparison with the results of Secs. II and III, the k_2 must exclude collisions involving $T_\pm$ states.

Note that if $k_{0,a}=k_{0,b}$, i.e., radicals a and b are produced in pairs, as well as recombine in pairs, while $k_{1,a}$ and $k_{1,b}$ are unimportant, then $n_a(t)=n_b(t)$. Also if identical radicals are formed and recombine, a single rate equation may be written in the usual manner, [although k_2 of Eq. (4.2) must be divided by two to avoid counting each collision twice]. The rate of change of the intensity may be expressed in terms of the different independent processes as

$$dI_a/dt=dI_a/dt]_{k_{0,a}}+dI_a/dt]_{k_{1,a}}+dI_a/dt]_{k_2}+dI_a/dt]_{T_{1,a}}. \tag{4.3}$$

The first term in Eq. (4.3) may be explicitly written as

$$dI_a/dt]_{k_0}=P_a^\infty(I)(dn_a/dt)_{k_{0,a}}=k_{0,a}P_a^\infty(I), \tag{4.4}$$

where $P_a^\infty(I)$ is the polarization generated from an initial S_0 (or T_0) state, which is itself generated by the radical-producing step.[26] (Note that if triplets are generated, then k_0 should refer only to the rate of production of T_0.) The next term in Eq. (4.3) is

$$dI_a/dt]_{k_{1,a}}=P_a(t)(dn_a/dt)_{k_{1,a}}=-k_{1,a}I_a(t). \tag{4.5}$$

The term due to the spin-selective rate equation is

$$dI_a/dt]_{k_2}=k_2n_a(t)n_b(t)\{P_a^\infty-\tfrac{1}{2}[P_a(t)-P_b(t)]\}, \tag{4.6}$$

where $P_a^\infty=\mathcal{P}\bar{P}_a^\infty$ is the unnormalized polarization after the collision (the duration of which is taken to a good approximation as being negligibly short, cf. Sec. III) and $P_a(t)$ its value just before collision. Equation (4.6) is written to include only those collisions that initially form S or T_0 states (and not $T_\pm$), since k_2 is the total rate constant for collisions initially forming only S or T_0 states; while $\frac{1}{2}[P_a(t)-P_b(t)]=2\,\mathrm{Re}\rho_{ST_0}(t)$ is the initial polarization associated with just the S–T_0 states [cf. Eq. (2.15), Ref. 13, and discussion below]. That is, Eq. (2.15) demonstrates that $P_a(t)$ may be split into a portion contributed by the S–T_0 states and another due to the $T_\pm$ states and the latter are unaffected by the collisions.

Note that more properly we must write $k_2=k_2[P_a(t),\ P_b(t)]$ and $P_a^\infty=P_a^\infty[P_a(t),\ P_b(t)]$ in Eq. (4.6),[27] expressing the fact that k_2 and P_a^∞ are functionals of $P_a(t)$ and $P_b(t)$. We now wish to point out that this functional dependence may often be neglected. The fraction of S–T_0 type collisions must be determined. A random encounter at time t between two radicals a and b will lead to density-matrix elements:

$$\rho_{a+,b-}=\tfrac{1}{4}[1-P_a(t)][1+P_b(t)] \tag{4.7a}$$

and

$$\rho_{a-,b+}=\tfrac{1}{4}[1+P_a(t)][1-P_b(t)] \tag{4.7b}$$

with no initial phase coherence between such states, (i.e., $\rho_{a+,b-;a-,b+}=0$). Then [cf. Eq. (2.15) and Ref. 13]

$$\rho_{S,S}(t)=\rho_{T_0,T_0}(t)=\tfrac{1}{4}[1-P_a(t)P_b(t)] \tag{4.7c}$$

$$\rho_{S,T_0}(t)=\tfrac{1}{4}[P_b(t)-P_a(t)]. \tag{4.7d}$$

Now usually $|P_a(t)|$ and $|P_b(t)|$ are very small compared to unity (i.e., <0.1) due in part to the T_1 process. Then to a good approximation

$$\rho_{S,S}(t)=\rho_{T_0,T_0}(t)\cong\tfrac{1}{4} \tag{4.8}$$

and k_2 simply refers to half of the total number of collisions, which is, for distinct radicals a and b, in Brownian motion theory[17,22,24]

$$k_2=2\pi dD. \tag{4.9}$$

Equations (4.7c) and (4.8) also show that random collisions between two radicals will always yield equal S and T_0 character, even if each radical has initial polarization. However, Eq. (4.7d) shows that there is an initial nonzero $\rho_{S,T_0}(t)$ due to this residual polarization [which has already been included in Eq. (4.6)]. The effect of such an initial state on P_a^∞ may be studied by means of our computer solutions of Sec. II. We have found such effects to be virtually negligible when $J_0>10^{10}$ sec^{-1} (with $D\lesssim10^{-5}$ cm^2/sec and $k>D/\Delta r^2$ sec^{-1}), due primarily to the fact that the initial polarization is quenched by spin exchange (but we will discuss

these matters in more detail elsewhere). Finally we have for the T_1 process[28]

$$dI_a/dt]_{T_{1,a}} = -n_a(t)[P_a(t)-P_{eq}]/T_{1,a}$$
$$= [-I_a(t)+n_a(t)P_{eq}]/T_{1,a}. \quad (4.10)$$

The total rate equation for the CIDEP intensity may then be written as

$$dI_a/dt = -I_a(t)[T_{1,a}^{-1}+k_{1,a}]-\tfrac{1}{2}k_2[n_bI_a(t)-n_aI_b(t)]$$
$$+[P_a^{\infty}(I)k_{0,a}+P_{eq}T_{1,a}^{-1}n_a(t)+k_2P_a^{\infty}n_a(t)n_b(t)] \quad (4.11)$$

with an equivalent expression for I_b. The steady state solution is

$$I_a^{SS} = \frac{[P_a^{\infty}(I)k_{0,a}+P_{eq}T_{1,a}^{-1}n_a^{SS}+k_2P_a^{\infty}n_a^{SS}n_b^{SS}]}{[T_{1,a}^{-1}+k_{1,a}+k_2n_b^{SS}\epsilon^{SS}]}, \quad (4.12a)$$

where $\epsilon^{SS}=\frac{1}{2}[1-n_a^{SS}I_b^{SS}/n_b^{SS}I_a^{SS}]$ and where n_a^{SS} and n_b^{SS} are obtained from Eq. (4.2). When, for simplicity, $k_{0,a}=k_{0,b}$ and $k_{1,a}=k_{1,b}$, then

$$n_a^{SS}=n_b^{SS}=[(k_1^2+4\mathfrak{F}k_2k_0)^{1/2}-k_1]2\mathfrak{F}k_2. \quad (4.12b)$$

The following are two specific cases we consider for comparison with recent experiments.

Case 1. The radicals are created by a light source and believed to be initially in a triplet state with initial polarization $P_a^{\infty}(I)$ as calculated in Sec. III. Also we assume that $n_a=n_b$ and $k_2n_b\ll k_1$, so that we may neglect the k_2 terms. The steady state solutions then become

$$n_a^{SS}=k_{0,a}/k_{1,a} \quad (4.13a)$$

and

$$I_a^{SS}=(P_a^{\infty}(I)T_{1,a}k_{0,a}+n_a^{SS}P_{eq})/(1+T_{1,a}k_{1,a}). \quad (4.13b)$$

Normally the experimental result is given as the measured enhancement V defined as the difference between the observed intensity and the intensity for a normal ESR experiment (i.e., without the CIDEP effect), divided by the latter. The normal ESR intensity I_{ESR} is obtained from Eq. (4.13b) by setting $P_a^{\infty}(I)=0$. By use of Eq. (4.13) we then obtain the following expression for the enhancement:

$$V=P_a^{\infty}(I)T_{1,a}k_{1,a}/P_{eq} \quad (4.14)$$

and the steady state intensity can then be written as

$$I_a^{SS}=I_{ESR}(1+V). \quad (4.15)$$

From Eq. (4.14) we see that the enhancement depends not only on $P_a^{\infty}(I)$, but also on $T_{1,a}$ and $k_{1,a}$ and that an increase of $k_{1,a}$ (decrease of the radical lifetime) will cause an increase in V. From Eq. (4.15) we see that V has to be less than -1 if the line should appear in emission.

Case 2. The radicals a and b are created at the same rate but without any initial polarization of importance. The radicals are supposed to react only by the selective chemical reaction. We also assume $T_{1,a}=T_{1,b}$ for simplicity. The steady state solutions now become

$$n_a^{SS}=n_b^{SS}=(k_0/\mathfrak{F}k_2)^{1/2} \quad (4.16)$$

and

$$I_a^{SS}+I_b^{SS}=2n_a^{SS}P_{eq} \quad (4.17a)$$

$$I_a^{SS}-I_b^{SS}=\frac{(2n_a^{SS}P_a^{\infty}\beta T_1/\mathfrak{F})}{(1+\beta T_1/\mathfrak{F})}, \quad (4.17b)$$

where β is the effective decay constant for the radicals given by

$$\beta=(k_0\mathfrak{F}k_2)^{1/2}. \quad (4.18)$$

We may again write the steady state intensity as Eq. (4.15) where, now, the enhancement V is given by (but cf. Ref. 26)

$$V=(I_a^{SS}-I_b^{SS})/(I_a^{SS}+I_b^{SS})$$
$$=\frac{P_a^{\infty}T_1\beta}{\mathfrak{F}P_{eq}(1+\beta T_1/\mathfrak{F})}. \quad (4.19)$$

Equation (4.19) is of the same form as Eq. (4.14) and similar conclusions may be drawn.

Comparison with Experiment. Fessenden[29] has recently performed some very interesting CIDEP experiments on several radical systems ($\dot{C}H_2CO_2^-$, $\dot{C}H(CO_2^-)_2$, $\dot{C}_6H_5OH$). He is able to demonstrate that the polarization must be due to the continuous regeneration of polarization by radical–radical reactions. He determines a quantity V_I that he calls the intrinsic enhancement. From our analysis of this section, we find this quantity to be equivalent to $P_a^{\infty}/\mathfrak{F}P_{eq}(1+\beta T_1/\mathfrak{F})\sim P_a^{\infty}/\mathfrak{F}P_{eq}$ [cf., Fig. 7(b)]. His values of V_I range from $\sim$30–100. Our results in Table II for $P_a^{\infty}(\text{asympt})/P_{eq}\mathfrak{F}$ range from 8–20 ($r_{ex}=4$ Å) and 15–35 ($r_{ex}=8$ Å) for $0.5\leq Q\times10^{-8}\leq4$ (Fessenden estimates $Q\sim10^8$ sec^{-1}) and $D=10^{-5}$ cm^2/sec. While our estimates are somewhat lower than Fessenden's experimental results, they are certainly of the correct order of magnitude, and this is encouraging.

Livingston[30] has seen substantial polarizations in the COOH·COH·ĊOH system, which he analyzes in terms of polarization generated at the radical-formation stage. An analysis of his preliminary results in terms of Eqs. (4.14) and (4.15) yield the very large values of $P_a^{\infty}/P_{eq}\sim$200–400, where his results for P_a^{∞} seem to depend on $k_{1,a}$. This would seem to indicate that a more detailed kinetic analysis is needed.

V. SUMMARY AND CONCLUSIONS

It has been demonstrated that, by the stochastic-Liouville method, one may rigorously predict CIDEP polarizations for reasonable types of models of the exchange interaction, the relative diffusive motion of

the interacting radicals, and spin-selective chemical reactions. The finite-difference technique employed in the present work permits rapid and convergent solutions without requiring untoward assumptions on the nature of the models, and the technique is readily employed to a variety of models.

The specific models considered for the exchange interaction included a contact exchange model as well as an exponentially decreasing $J(r)$ with r. The latter, more realistic model, was shown to yield distinctly different behavior from the former in that for $J_0 > 10^{12}$ sec^{-1} the polarization levels off to a substantial asymptotic value P^∞(asympt), which is greater the slower the decrease of $J(r)$ with r. This feature is not obtained for the contact exchange model, where P_a^∞ rapidly goes to zero for $J_0 > 10^{12}$ sec^{-1}, demonstrating that this (frequently used) simple model is not really adequate for proper descriptions of the CIDEP phenomenon. The polarizations are, in general, functions of $J(r)$, Q (half the difference in ESR resonant frequencies between the radical pair), D (the diffusion coefficient), and k (the rate of spin-selective chemical reactions) and these dependences have been detailed. In particular the dependence of P_a^∞ on Q varies with D and ranges from $P_a^\infty \propto Q$ for very fast diffusion and $Q \sim 10^8$ sec^{-1} (when maximum re-encounter distances of $\sim$200 A are utilized); to $P_a^\infty \propto Q^{1/2}$ for normal liquid diffusion rates; to $P_a^\infty \propto Q^\epsilon$ where $\frac{1}{2} < \epsilon < 0$ for very slow diffusion and large Q. An interesting result in the case of a spin-selective chemical reaction is that the S–T_0 mixing can actually enhance the fraction of radicals that react per "collision." Another interesting result for the spin-selective (random initial condition) case is that the quantity $P_a^\infty/\mathfrak{F}$, where $\mathfrak{F}$ is the recombination probability per collision, is independent of the recombination rate k when $J_0 > 10^{10}$ sec^{-1} (for $D \approx 10^{-5}$ cm^2/sec).

In our analysis of CIDEP intensities, the polarizations P_a^∞ have been related to what can actually be observed for typical schemes of radical production, reaction, and relaxation. In general, the signal enhancement depends on a product of P_a^∞, with the spin-lattice relaxation time T_1 and the radical decay rate compared to the equilibrium polarization. We are able to predict values of $P_a^\infty/\mathfrak{F}$ that are of the correct order of magnitude compared to recent experimental results of Fessenden and this encourages us in the belief that the basic CIDEP mechanism is reasonably well understood.[31]

The application of our methods to an analysis of CIDNP and Heisenberg-spin exchange will be discussed elsewhere.

ACKNOWLEDGMENTS

We wish to thank R. W. Fessenden and R. Livingston for communication of their results prior to publication.

* Supported in part by the National Science Foundation (Grant GP-13780) and the Materials Science Center, Cornell University.

† Present address: Chemistry Department, University of Aarhus, 8000 Aarhus C, Denmark.

[1] J. B. Pedersen and J. H. Freed, J. Chem. Phys. **57,** 1004 (1972).

[2] (a) R. Kubo, Adv. Chem. Phys. **16,** 101 (1969); J. Phys. Soc. Jap. Suppl. **26,** 1 (1969); (b) J. H. Freed, G. V. Bruno, and C. F. Polnaszek, J. Phys. Chem. **75,** 3385 (1971); J. Chem. Phys. **55,** 5270 (1971); (c) J. H. Freed, in *ESR Relaxation in Liquids*, edited by L. T. Muus and P. W. Atkins (Plenum, New York, 1972).

[3] J. H. Freed, Annu. Rev. Phys. Chem. **23,** 265 (1972).

[4] R. Kaptein and J. L. Oosteroff, Chem. Phys. Lett. **4,** 195 (1969); R. Kaptein, Ph.D. Thesis, Leiden, 1971.

[5] H. Fischer, Chem. Phys. Lett. **4,** 611 (1970).

[6] S. H. Glarum and J. H. Marshall, J. Chem. Phys. **52,** 5555 (1970).

[7] F. J. Adrian, J. Chem. Phys. **54,** 3918 (1971).

[8] P. W. Atkins, R. C. Gurd, K. A. McLauchlan, and A. F. Simpson, Chem. Phys. Lett. **8,** 55 (1971).

[9] F. J. Adrian, Chem. Phys. Lett. **10,** 70 (1971).

[10] It is possible to include the effects of intermolecular charge and exchange interactions on the diffusion process by means of the stochastic-Liouville approach particularly for the finite difference method utilized here. These matters will, however, be discussed elsewhere, J. B. Pedersen and J. H. Freed (unpublished).

[11] The fact that Γ_Ω does not appear in Eq. 2.9 may be easily seen by first expanding $\rho(\mathbf{r}, t)$ in eigenfunctions of Γ_Ω [i.e., spherical harmonics $Y_M{}^L(\theta, \phi)$]. The integration of Eq. (2.8) will only leave the $Y_0{}^0(\theta, \phi)$ term, but $\Gamma_\Omega Y_0{}^0 = 0$.

[12] (a) H. S. Carslaw and J. C. Jaeger, *Conduction of Heat in Solids* (Oxford U. P., London, 1959). (b) J. B. Pedersen in *ESR Relaxation in Liquids*, edited by L. T. Muus and P. W. Atkins (Plenum, New York, 1972).

[13] It is often useful to interconvert between density-matrix elements in the S, T_0, $T_\pm$ representation and those in the product representation of doublet pairs, which we write as $\rho_{+a,-b;+a-b} = \rho_{+a-b;\ +a,-b;-a+b}$, etc. The relationships are easily obtained in the usual way, and we give the important ones here for convenience:

$$\rho_{T\pm,T\pm} = \rho_{a\pm,b\pm},$$

$$\rho_{T_0,T_0} = \tfrac{1}{2}(\rho_{+a,-b} + \rho_{-a,+b}) + \mathrm{Re}\rho_{+a,-b;-a+b},$$

$$\rho_{S,S} = \tfrac{1}{2}(\rho_{+a,-b} + \rho_{-a,+b}) - \mathrm{Re}\rho_{+a,-b;-a+b},$$

$$\rho_{S,T_0} = \tfrac{1}{2}(\rho_{+a,-b} - \rho_{-a,+b}) + i\mathrm{Im}\rho_{+a,-b;-a,+b}.$$

Also:

$$\rho_{\pm a,\mp b} = \tfrac{1}{2}(\rho_{S,S} + \rho_{T_0,T_0}) \pm \mathrm{Re}\rho_{S,T_0},$$

$$\rho_{+a,-b;-a,+b} = \tfrac{1}{2}(\rho_{T_0,T_0} - \rho_{S,S}) + i\mathrm{Im}\rho_{S,T_0}.$$

[14] G. E. Roberts and H. Kaufman, *Tables of Laplace Transforms*, (Saunders, Philadelphia, 1966).

[15] J. M. Deutch, J. Chem. Phys. **56,** 6076 (1972).

[16] (a) Even within a finite difference approach in the variable r, one could first solve for the eigenvectors (and eigenvalues) of the $\mathbf{W}$ matrix Eq. (2.22) and then rewrite Eq. (2.31) in this new representation. We have not done this in part because 1) $\varrho(0)$ is rendered more complex for our cases, and 2) for arbitrary variation of $J(r)$ with r, $\mathcal{H}^z$ in the combined spin and r space becomes more complex (cf. Ref. 3). It may be noted that such an approach should be equivalent to first Fourier transforming from r to k space, then expanding $\hat{\rho}(k, s)$ in eigenfunctions of the diffusion operator, and then using finite difference methods. (b) The matrix of Eq. (2.34) can readily be diagonalized, yielding eigenvalues $\lambda = 0, \pm[J(r)^2 + Q^2]^{1/2}$. All three eigenvectors are functions of r, so such a diagonalization would introduce "nonadiabatic" couplings into the $\tilde{\mathbf{W}}$ (cf. Ref. 3). We have chosen to avoid this complication.

[17] S. Chandrasekhar, Rev. Mod. Phys. **15,** 1 (1943).

[18] N. Bloembergen and Y. R. Shen, Phys. Rev. **133,** A37 (1964).

[19] Copies of our program are available upon request.

[20] We have obtained improved convergence over Ref. 1. The trends reported there are generally in agreement with those reported here (although there are numerical changes), but the Δr dependence and results for slow diffusion ($D \lesssim 10^{-6}$ cm^2/sec)

needed revision. Therefore, the accurate results reported in this work should be utilized.

[21] (a) A useful check on the diffusional portion of the program (and the boundary conditions) is to use the fact that, $F_{i,j} = r_j/r_i$,[15] (i.e. the probability that particles separated by r_i will diffuse to r_j). When there is a very fast chemical reaction at r_0 (i.e., $k\Delta r^2 \gg D$), one may write for F, the fraction of particles started at r_k such that $r_0 < r_k < r_N$ which react: r_0/r_k; but since r_N is finite and particles reaching r_N are absorbed, the fraction must be corrected to $r_0/r_k - (r_0/r_N)\mathcal{P} = (1-\mathcal{P})$. The computed results for $\mathcal{P}$, do give excellent agreement with this expression. (b) Note that $\Phi(x, \sigma) \equiv \int \Phi(x, \tau) e^{-\tau\sigma} d\sigma$ obeys the equation $\sigma\Phi(x, \sigma) - \Phi(x, 0) = [-i(d^2/D)\mathcal{K}^x(x) + \partial^2/\partial x^2]\Phi(x, \sigma)$ with initial condition $\Phi(x, 0) = (1+x)\rho(r, 0)$ and

$$\rho(t) = \int_0^\infty d^3(x+1)\Phi(x, \tau)dx.$$

[22] I. Amdur and G. G. Hammes, *Chemical Kinetics* (McGraw-Hill, New York, 1966), Chap. 2.

[23] M. Eigen, Z. Physik. Chem. Neue Folge **1**, 176 (1954).

[24] M. P. Eastman, R. G. Kooser, M. R. Das, and J. H. Freed, J. Chem. Phys. **51**, 2690 (1969).

[25] Note that the functional form of Eq. (3.2) cannot be predicted by perturbative methods, involving J as a perturbation, cf. Refs. 24 and 2(c).

[26] Note that more rigorously, Eq. (4.4) should be written in a form recognizing that the radicals may have hyperfine structure [cf. Eqs. (2.3) and (2.4)], and one is interested in the intensity of a particular (ith) hyperfine line. Then Eq. (4.2) become $I_{a_i} = n_{a_i} P_{a_i}$ and Eq. (4.4) would more correctly be written as

$$\left.\frac{dI_{a_i}}{dt}\right]_{k_{0,i}} = p_{a_i} k_{0,a} \sum_j p_{b_j} P_a^\infty(I, Q_{i,j}) \equiv p_{a_i} k_{0,a} P_a^\infty(I, Q_i.\text{Av}),$$

where p_{a_i} and p_{b_j} are the normalized probabilities that radicals a and b are respectively associated with the ith and jth hyperfine levels; also $Q_{i,j}$ is the associated value from Eq. (2.30), and the functional dependence of P_a^∞ on $Q_{i,j}$ is indicated. We have not explicitly done this in order to retain simplicity in illustrating the main points.

[27] Note here that this term should be

$$p_{a_i} k_2 n_a(t) n_b(t) \sum_j \{p_{b_j} P_a^\infty[Q_{i,j}, P_{a_i}(t), P_{bj}(t)] - \tfrac{1}{2}[P_{a_i}(t) - P_{b_j}(t)]\},$$

while the first order term of Eq. (4.5) should be $-P_{a_i} k_{1,a} I_{a,i}$, cf. Ref. 26.

[28] If we were considering properly the detailed hyperfine structure of the radicals, one would require, in general, coupled relaxation expressions amongst the hyperfine levels, cf. J. H. Freed, J. Chem. Phys. **43**, 2312 (1965). When simple symmetry relations exist for the requisite transition probabilities (e.g., only pure nuclear-spin-flip terms and no cross-flips involving simultaneous electron–nuclear flips), then these coupled relaxation expressions may be conveniently formulated in terms of the P_{a_i} (i.e., the differences between the $m_s = +$ and $-$ states for each nuclear configuration), cf. Ref. 24 and J. H. Freed, D. S. Leniart, and H. D. Connor, J. Chem. Phys. (to be published).

[29] R. W. Fessenden, J. Chem. Phys. (submitted).

[30] R. Livingston (private communication).

[31] Adrian [J. Chem. Phys. **57**, 5107 (1972)] has recently estimated CIDEP intensities using an interesting but approximate approach. His tabulated results (given for large J_0 values) do *not* display the kind of functional dependences found in our work, although they are of comparable order of magnitude.